

# Optimization of a Vertical Axis Micro Wind Turbine for Low Tip Speed Ratio Operation

Ryan McGowan, Kevin Morillas, Akshay Pendharkar, and Mark Pinder

*The Daniel Guggenheim School of Aerospace Engineering  
Georgia Institute of Technology, Atlanta, GA, 30332, United States*

Dr. Narayanan Komerath

*The Daniel Guggenheim School of Aerospace Engineering  
Georgia Institute of Technology, Atlanta, GA, 30332, United States*

This paper describes progress on a vertical axis wind turbine (VAWT) testbed aimed at the needs of a single family. VAWTs are potentially better suited than the more common horizontal axis wind turbine (HAWT) to meet the energy needs of homes and villages because of lower blade speeds and more benign failure modes; however, they are also more complex in operation. The testbed described here is intended to investigate various technologies for construction and operation and to optimize the value of such turbines as mass-market devices. The methods of analysis, simulation, design, construction, and control draw on classical as well as leading-edge aerospace technologies.

## Nomenclature

$c$	Chord
$c_d$	Section drag coefficient
$c_l$	Section lift coefficient
$C_P$	Power coefficient
$C_n$	Normal coefficient
$C_t$	Tangential coefficient
$n_a$	Number of arms
$n_b$	Number of blades
$P$	Power
$r$	Radius
$Re$	Reynolds number
$T$	Torque
$U_t$	Tangential velocity
$U_\infty$	Freestream velocity
$W$	Weight
$\alpha_b$	Blade angle of attack
$\alpha_g$	Guide vane angle of attack
$\theta_b$	Blade azimuth angle
$\lambda$	Tip speed ratio
$\sigma$	Solidity
$\omega$	Angular velocity

## I. Introduction

Vertical axis wind turbines offer a safe, inexpensive solution for off-grid power generation in remote areas. They can be located closer to the ground than horizontal axis machines. The rotational speeds and blade stresses are much lower than those on horizontal axis machines of the same power level, and hence blade technology can be brought down to levels that are compatible with construction and maintenance using locally available skills and materials. However, the VAWT is a complex machine with low efficiency, operating with unsteady aerodynamics and strong interactions between the flows around its components. VAWT operating characteristics are also highly complex. These machines cannot start themselves except through drag-based devices and cannot reach optimal operating speeds without external drives. Their power generation depends very strongly on the tip speed ratio, the ratio of blade speed to wind speed. Optimal operation typically occurs at tip speed ratios between 3 and 5, meaning that the turbine speed must exceed wind speed by a large factor. To reach such speeds, a motor is typically used. For optimal operation, the control system must then reverse the direction of power flow from motor to generator mode and keep the machine in a viable tip speed ratio regime. To make the device suitable for its intended role, these operations must become routine and adapt to the local environment. Such a state of technical development requires a thorough understanding of all aspects of machine characteristics.

The objective of the work described in this paper is to develop a VAWT testbed that can be used to enable prediction and optimization of such machines. Progress towards this objective has taken a meandering path.<sup>1</sup> A constraint imposed at the beginning was that all rotating parts (which are typically very expensive to buy in remote locations) were to be obtained exclusively from bicycles, or at most, motorcycles. Both of these vehicles are freely available in most parts of the world, and their operation and maintenance are familiar to local people—even children—of all socioeconomic levels. Initial designs studied the possibility of using blades that were highly flexible and had very simple geometry. Vertical window blind slats were used as blades, their camber providing some slight bending stiffness. Given that the blades were to be inexpensive, we investigated the possibility of using double blades arranged in biplane fashion as a way to increase power output without substantially increasing the solidity or the number of arms. An aluminum double blade attachment was invented to hold the cambered, thin-plate blinds at the top and bottom. A version with four double blades was initially tested in a low-speed wind tunnel but quickly changed to three double blades to avoid sub-harmonic swaying of the mast. Both the three-bladed and four-bladed versions exhibited a torque well in the azimuth range between  $90^\circ$  and  $180^\circ$  (where the blade was advancing into the wind) due to blade stall. This prevented self-starting even when Savonius-type drag tubes were added. This problem was resolved by adding a static guide vane in this azimuth range to redirect the wind. A  $1\text{ m} \times 1\text{ m}$  model reached over 250 rpm in wind speeds up to 45 ft/s at the exit of an open-return low speed wind tunnel. Centrifugal bowing of the blades was controlled by tying the blades to the mast in the middle using nylon threads. A  $2\text{ m} \times 2\text{ m}$  version was then developed using the same technology of vertical blinds and tested in the settling section of a closed-return tunnel, where there were still strong fluctuations in the wind downstream of the tunnel fan blades. This experiment failed completely, as the blinds proved to have too little torsional stiffness and fluttered out of control as the machine began to turn, driven by the drag tubes. In both this and the  $1\text{ m} \times 1\text{ m}$  version, the peak speed reached actually increased when the lift-generating blades were removed and the machine was operated with only Savonius drag tubes. The upper and lower arm assemblies were then rotated  $30^\circ$  with respect to each other to slant the blades and thus distribute the power generation more evenly. The blades were built with low Reynolds number airfoil sections, wooden ribs, a PVC pipe as the main spar, and PVC roof-flashing sheets wrapped over the templates and stapled at the trailing edge to form the torsion box and skin. The attachments were PVC tube T-joints, thereby keeping the construction technology and parts availability at the desired levels. This version generated mechanical power levels of over 60 W in strong winds. A larger model 6 ft in diameter was then developed, this time intended to survive high wind speeds in a  $2.54\text{ m} \times 2.74\text{ m}$  wind tunnel. This is ultimately intended for use by coastal communities and designed to survive winter winds. Accordingly the construction used heavier steel parts and blades constructed with wood, high-density foam, and fiberglass/resin skins.

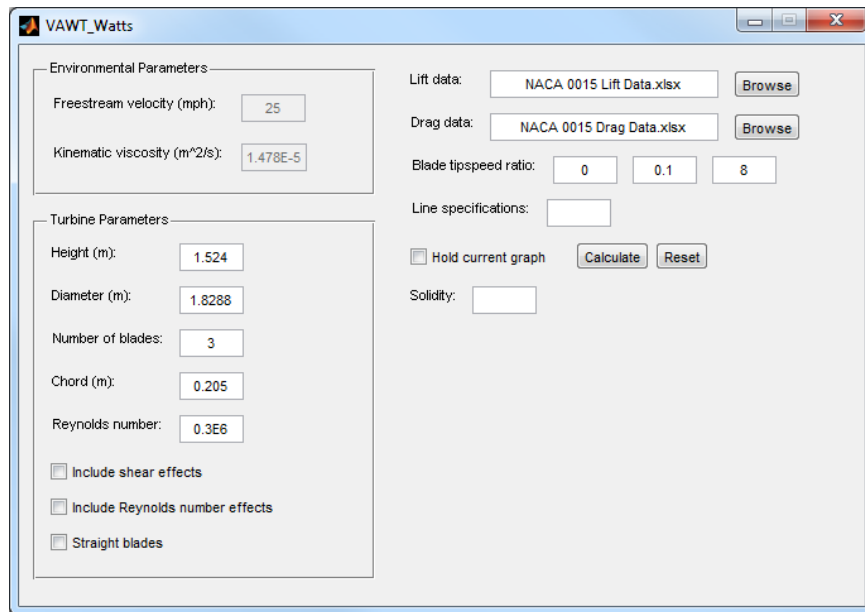


Figure 1. VAWT simulation GUI.

## II. Simulation

Computational models were developed to predict the performance of vertical axis micro wind turbines. An initial model sought to predict how the 6 ft VAWT would accelerate and reach equilibrium in a given freestream velocity.<sup>1</sup> It used the single streamtube method developed by Templin,<sup>2</sup> assuming isolated blades with no streamtube interactions. The blade Reynolds number was assumed to be constant through the cycle. Kirke<sup>3</sup> shows that these assumptions cause substantial errors at low Reynolds numbers. A refined model used the multiple streamtube method developed by Strickland<sup>4</sup> which accounts for energy extraction, calculating a disk velocity less than the freestream velocity and determining the Reynolds number as a function of position. Multiple streamtube theory splits the turbine into several streamtubes along the horizontal and vertical axes which allows the effects of variations in disk velocity and shear to be included. An induction factor is found iteratively and a local power coefficient computed for each streamtube. The essence of Strickland's DART code was translated from FORTRAN into MATLAB, with a GUI enabling the user to specify the configuration of the VAWT. The user can choose the turbine dimensions and blade geometry by inputting the parameters to the GUI shown in Figure 1. Finally, a simulation based on cascade theory<sup>5</sup> may give still better results: According to Islam et al.,<sup>6</sup> "The Cascade model can predict the overall values of both low and high solidity turbines quite well," and "[t]he instantaneous blade forces calculated by this model show improved correlation in comparison to those calculated by the conventional Momentum model."

The three-armed VAWT was simulated with the capability to incorporate double blades, a guide vane, and drag tubes for self-starting and operation at low tip speed ratios. The performance of the model was validated against predictive models and data from the literature.<sup>1</sup> It was shown that using low Reynolds number data improved the correlation with experiments substantially at low tip speed ratios. The results also showed that high solidity brings down the tip speed ratio required for peak power coefficient while lowering the peak power coefficient itself at very low tip speed ratios. This agrees with the trend observed by Strickland<sup>4</sup> and reproduced in Figure 2. The trends from the calculations are compared to those from the literature in Figures 3 and 4.

### II.A. Drag Channels and Reynolds Number Effects

Simple drag channels made by splitting a round tube down its diameter were modeled as drag generators, with the drag coefficient interpolated sinusoidally between 2.30 when the concave side faces the wind and 1.20 when the cylinder surface faces the wind. Similar to a Savonius wind turbine, these drag tubes provide a simple way to generate torque at low turbine speeds when the blade aerodynamics do not generate any lift-

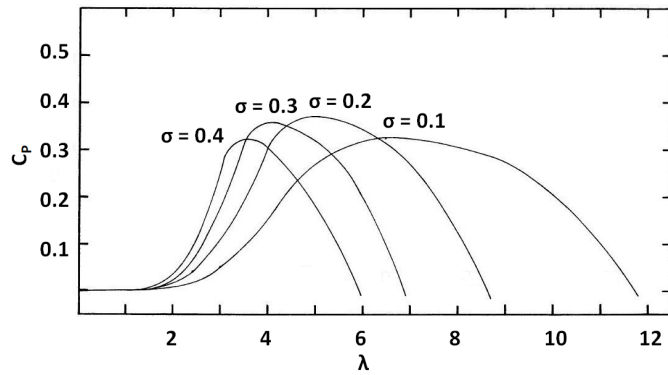


Figure 2. Power coefficient vs. tip speed ratio for various solidities (Sandia).<sup>4</sup>

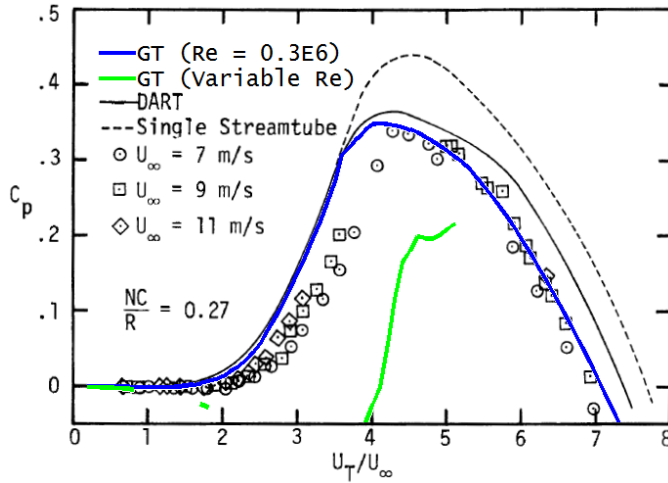


Figure 3. Comparison of Georgia Tech and Sandia performance predictions at 0.27 solidity.

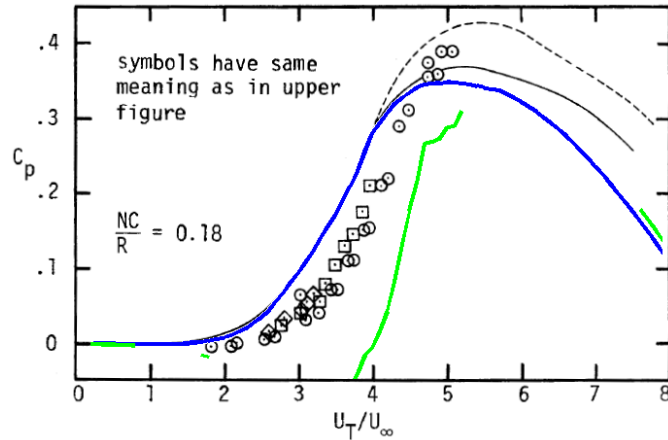


Figure 4. Comparison of Georgia Tech and Sandia performance predictions at 0.18 solidity.

based torque. Low Reynolds number blade aerodynamic data were interpolated from Sheldahl and Klimas.<sup>7</sup> Below Reynolds numbers of 10,000 data are not available, and in this region constant Reynolds number was assumed, improving correlation with predicted power curves from Sandia<sup>4</sup> as shown in Figures 3 and 4. The dashed black line is the Sandia performance prediction utilizing single streamtube theory, while the solid line is the Sandia performance prediction utilizing multiple streamtube theory.

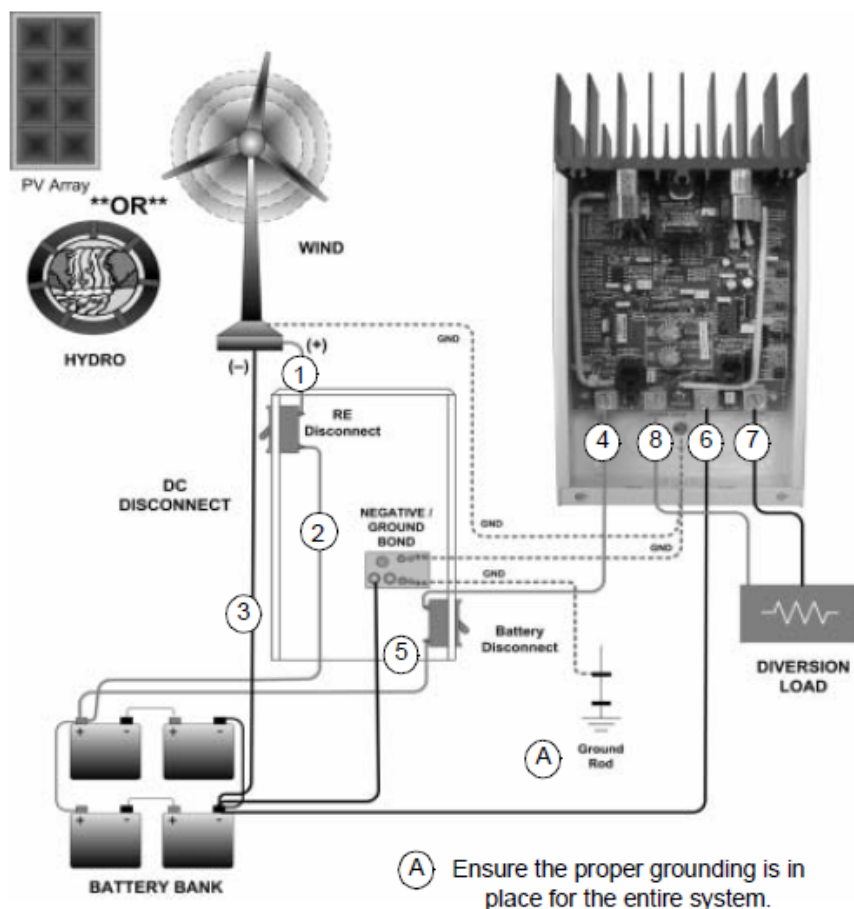


Figure 5. Diversion control mode wiring.

### III. Experimental Setup

#### III.A. Belt Drive

A V-belt drive was used to transfer power between the turbine shaft and the motor-generator shaft. Ideally, the pulley on the turbine shaft would be larger than that on the motor-generator shaft when the turbine is running the motor and vice versa when the motor is running the turbine. However, since it was deemed too complicated/expensive to implement a mechanism for changing gears automatically, a gear ratio of 1:1 was used.

#### III.B. Charging Circuit

The use of a motor-generator to run the turbine up to operating speed requires changes to be made to the typical charging circuit, since most manufacturers of renewable energy (RE) charge controllers assume a turbine will be purely wind-powered. Figure 5 shows the original circuit which was modified in order to run the motor off of the battery bank. The charge controller does not regulate the voltage to the battery when in diversion control mode. Instead, it only monitors the voltage of the battery and switches the circuit to the dump load when it sees that the battery is fully charged. When this happens, excess energy will be diverted to the diversion load and dissipated as heat. A pair of fuses was used to protect the battery and sensitive components from spikes in voltage and current. The switches in Figure 5 can be used to manually disconnect the motor from the battery and/or the battery from the charge controller.

To keep the turbine spinning in the same direction regardless of whether the motor is running the turbine or vice versa, a DPDT switch has been included in the circuit. Figure 6 shows the modified circuit in the charging configuration; the DPDT switch is in the upper left portion of the image. When both the renewable

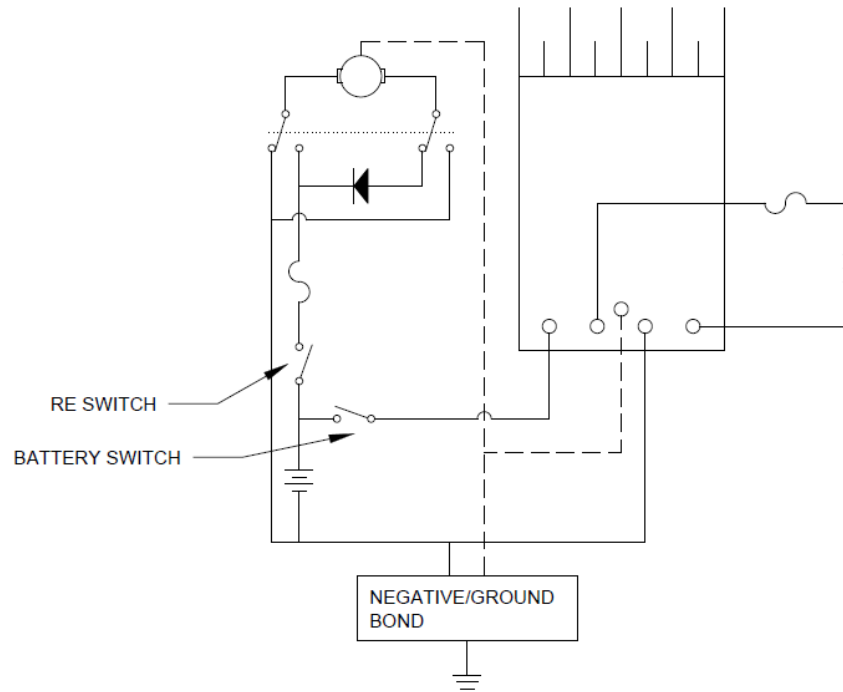


Figure 6. Modified circuit.

energy and battery switches are closed, the current will flow clockwise, and the VAWT will start charging the battery by running the motor-generator. If the battery has a higher voltage than the motor-generator, the diode will prevent it from running the motor. On the other hand, when the VAWT is experiencing trouble self-starting, the DPDT switch is flipped to the run position, and the battery switch is opened. The current will flow counterclockwise, and the motor-generator will run the shaft, spinning the turbine up to the optimum tip speed ratio. Once the optimum tip speed ratio is reached, the DPDT switch can be flipped back to the charging position, and the battery switch can be closed again.

### III.C. Rope Brake Dynamometer

A rope brake dynamometer was used to test the power output of the wind turbine model in a low speed wind tunnel, where the wind speed can be made steady and uniform. The setup consisted of a rope which was wrapped around a pulley on the bottom of the turbine; this rope was fixed on one end and held a weight on the other as shown in Figure 7. By recording the torque from the weight as well as the angular velocity of the turbine when subjected to a given freestream velocity, power was determined from Equations (1) and (2).

$$T = Wr \tag{1}$$

$$P_{mechanical} = T\omega \tag{2}$$

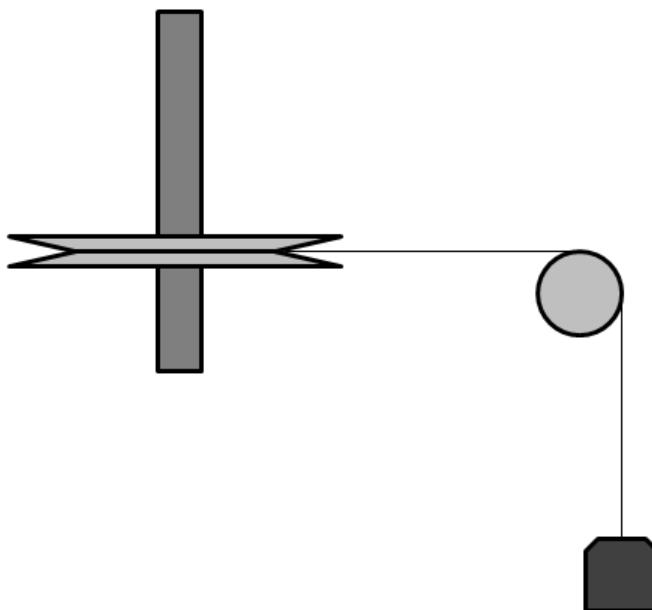


Figure 7. Rope brake dynamometer.

## IV. Results

### IV.A. Low Tip Speed Ratio Wind Tunnel Tests

During testing, the maximum tip speed ratio reached by the 6 ft VAWT was only 0.6. However, the predicted  $C_P$  curve generated by the VAWT simulation indicates that peak efficiency is not reached until the turbine is spinning at a tip speed ratio of almost 3. From the wind tunnel testing, it is obvious that the turbine is not capable of reaching such a tip speed ratio on its own (at least not in safe weather conditions), but one solution is to attach a motor or some other drive system to the turbine which spins it up to the necessary speed before shutting off. Indeed, this approach is taken by many manufacturers of wind turbines facing similar problems.

If the turbine is to be operated at tip speed ratios higher than 0.6, then it is imperative that improvements in structural stability be made. It is also a good idea to incorporate a safety brake which would prevent the turbine from running at unsafe speeds. Disturbing shaking of the turbine was noticed even at a tip speed ratio of 0.6; higher angular velocities could very well lead to turbine damage and injury of nearby people. In addition to ensuring the turbine is evenly balanced, adding more blades can smooth the variation in forces and torques, but this comes with its own set of tradeoffs (particularly the increase in solidity).

### IV.B. Charging Circuit Tests

The charging circuit was attached to the  $1\text{ m} \times 1\text{ m}$  turbine, and a rough calculation of the motor-generator rpm was performed through video analysis. The VAWT was switched on and allowed to accelerate until the maximum constant rpm was reached. The video was slowed to one tenth of the real time speed because it was easier to find the time taken for a full rotation. This time was approximately 5 s at one-tenth speed and so at normal speed, the turbine blades made a full rotation in half a second. Therefore, the angular velocity was calculated to be approximately 120 rpm. An optical encoder will be used to make more accurate measurements of the rpm, while a digital oscilloscope will be used to record the voltage across the motor.

The construction and implementation of such a charging circuit proves that a motor-generator drive is effective in accelerating the turbine out of dead zones. However, if the freestream velocity is greater than 6.3 ft/s, it is not possible to accelerate the 6 ft VAWT to the operating tip speed ratio of 3 without using a gear ratio other than 1:1. Future work may focus on developing a method of switching gears which is not prohibitively complicated and expensive.

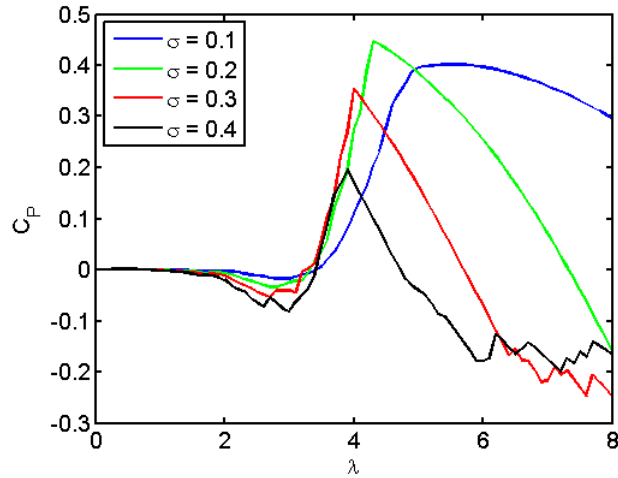


Figure 8. Power coefficient vs. tip speed ratio for various solidities of the 3 ft VAWT ( $U_\infty = 12$  m/s,  $\lambda = 1$ ).

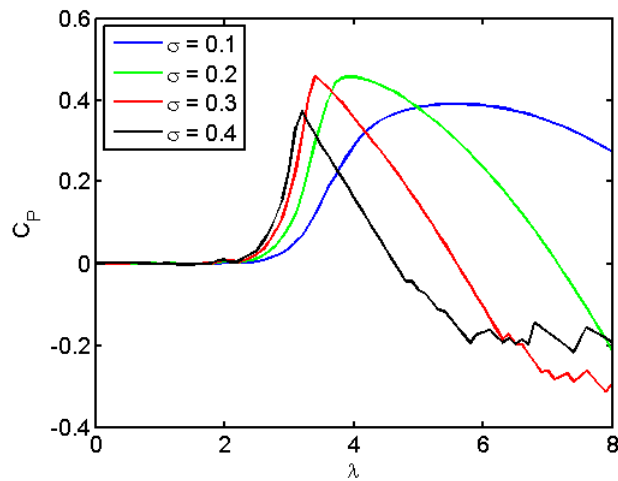


Figure 9. Power coefficient vs. tip speed ratio for various solidities of the 6 ft VAWT ( $U_\infty = 12$  m/s,  $\lambda = 1$ ).

## IV.C. Momentum Theory

### IV.C.1. Single Streamtube Theory

Using the single streamtube code on the 6 ft VAWT, the current power prediction for a freestream velocity of 25 mph and a tip speed ratio of 3 is approximately 387 W. Dividing by the total wind power available gives a power coefficient of 0.17. The calculated power coefficient satisfies Betz's Law, though it is known that VAWT simulations based on single streamtube theory tend to overestimate the power output.

### IV.C.2. Multiple Streamtube Theory

The multiple streamtube code gives a more pessimistic power coefficient of 0.07 for a freestream velocity of 25 mph and a tip speed ratio of 3. It is also interesting to note the role solidity plays in power generation. Calculating solidity as  $n_a c/r$ , the 6 ft VAWT has a relatively high solidity of 0.67. As can be seen from Figures 8 and 9, the shape of the power coefficient curve is much more erratic when the VAWT has a higher solidity; when the chord length has been modified to lower the solidity, the  $C_P$  vs.  $\lambda$  curve exhibits the expected shape.

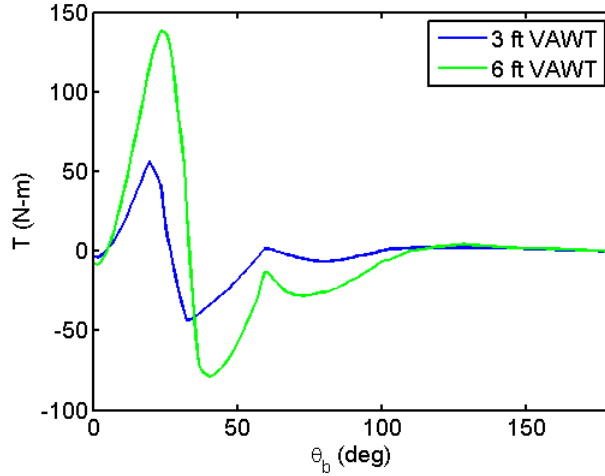


Figure 10. Simulated variation of torque with blade azimuth angle ( $U_\infty = 12$  m/s,  $\lambda = 1$ ).

## V. Sources of Inefficiency

### V.A. Negative Torque

From Figure 10, it can be seen that the torque acting on a blade becomes negative for a significant portion of each revolution—that is, the forces on that blade tend to act in a direction opposite to the turbine’s motion. The turbine will not self-start unless the net torque (and consequently the power coefficient) is positive for all tip speed ratios up to the operating condition.<sup>3</sup>

In any case, negative torque even on one blade does counteract the motion of the turbine and hinders energy production. Ideally, the tangential coefficient would remain positive over one complete revolution, but this is not easily achieved. Looking at Equation (3), one obvious option is to choose an airfoil which has higher lift coefficients and lower drag coefficients. Alternatively, the angle of attack can be varied by incorporating a pitching mechanism or even changing the direction of the relative velocity felt by the blades. Here the goal would be to maximize  $\sin \alpha_b$  and minimize  $\cos \alpha_b$  when  $c_l$  is positive, and vice versa when  $c_l$  is negative. (The lift coefficient of a symmetric airfoil becomes negative for angles of attack from  $90^\circ$  to  $180^\circ$  and  $270^\circ$  to  $360^\circ$ .) Figure 11 shows that for a NACA 0015 airfoil, the tangential coefficient is at its maximum for an angle of attack of approximately  $12^\circ$ . Of course, the use of guide vanes to keep the blade angle of attack at  $12^\circ$  introduces additional complexity, so the benefits must be weighed against the extra costs as well as difficulties in manufacturing and maintenance.

$$C_t = c_l \sin \alpha_b - c_d \cos \alpha_b \quad (3)$$

As seen in Figure 12, varying the tip speed ratio may change the location and magnitude of the positive and negative peaks but does not completely remove or improve negative torque regions. Figure 13 shows a more promising solution to this problem. In this figure, the variation of torque is plotted against azimuth location for various guide vane angles of attack, giving insight as to how the freestream should be rotated to remove negative torque. Realistically, there would be large losses associated with turning the flow at these angles; however, this simulation does provide a specific solution.

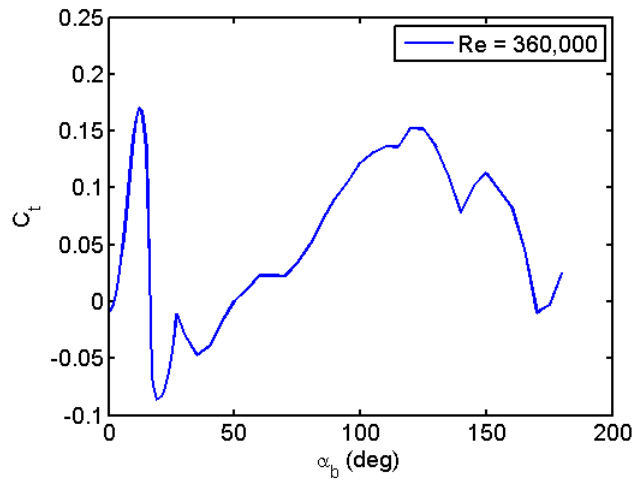


Figure 11. Tangential coefficient vs. blade angle of attack for a NACA 0015 airfoil.

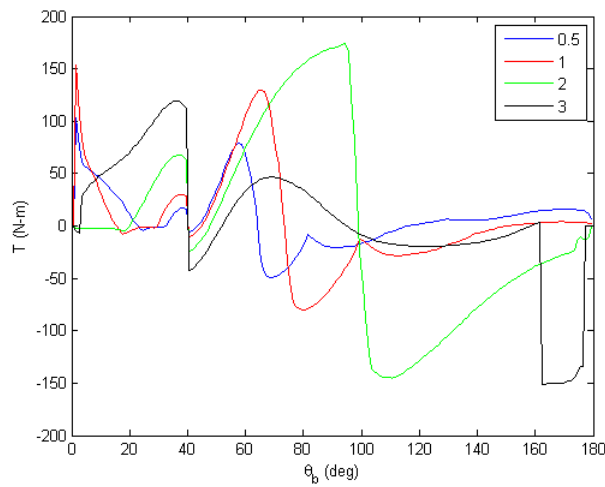


Figure 12. Torque vs. blade azimuth angle for various tip speed ratios ( $U_\infty = 12$  m/s,  $\alpha_g = -40^\circ$ ).

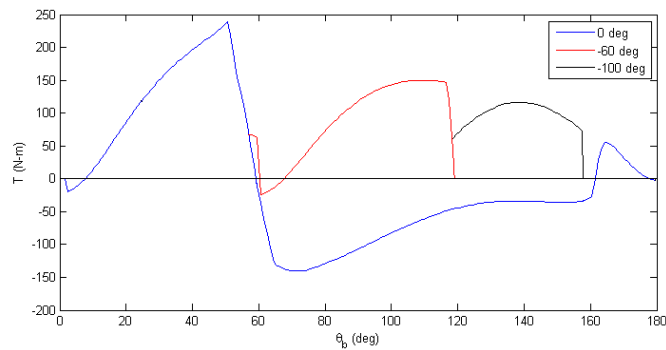


Figure 13. Torque vs. blade azimuth angle for various guide vane angles of attack of the 6 ft VAWT ( $U_\infty = 12$  m/s,  $\lambda = 2$ ).

## VI. Conclusion

In this paper we have begun to integrate prediction, design, and testing of a  $2\text{ m} \times 2\text{ m}$  vertical axis wind turbine with slanted double blades. Predictions of the operating points incorporating multiple streamtube

theory and accounting for interactions are validated against published results elsewhere. Reynolds number effects are clearly seen in the predictions, and their proper inclusion allows the predictions to match experimental data extremely well. A self-starting device using drag tubes is included in the simulation. It is seen that the vertical axis wind turbine must operate at a tip speed ratio that is substantially greater than 1. Limiting the turbine speed for safety implies that high tip speed ratio is best achieved at low wind speeds by taking the turbine to a good operating speed using human pedaling action or an electric motor. This will allow extraction of substantial amounts of power from the wind compared to what we have been able to achieve using purely self-powered machine operation. With this state of predictions we are in a position to go to detailed time-resolved simulations and thus to control algorithms for adapting to given wind patterns and optimizing power extraction and safety.

## Acknowledgments

This study was enabled by NASA Grant NNX09AF67G S01, the EXTROVERT initiative to develop resources for cross-disciplinary innovation. Mr. Tony Springer is the technical monitor.

## References

- <sup>1</sup>Komerath, N. M., "Prediction and Validation of a Micro Wind Turbine for Family Use," *Proceedings of the IMETI Conference*, Orlando, FL, July 2011.
- <sup>2</sup>Templin, R. J., "Aerodynamic Performance Theory for the NRC Vertical-Axis Wind Turbine," *NASA STI/Recon Technical Report N*, Vol. 76, 1974, pp. 16618.
- <sup>3</sup>Kirke, B. K., *Evaluation of Self-Starting Vertical Axis Wind Turbines for Stand-Alone Applications*, Ph.D. thesis, Griffith University, 1998.
- <sup>4</sup>Strickland, J. H., "The Darrieus Turbine: A Performance Prediction Model Using Multiple Streamtubes," Report SAND75-0431, Sandia National Laboratories, October 1975.
- <sup>5</sup>Hirsch, H. and Mandal, A. C., "A Cascade Theory for the Aerodynamic Performance of Darrieus Wind Turbines," *Wind Engineering*, Vol. 11, No. 3, 1987, pp. 164–175.
- <sup>6</sup>Islam, M., Ting, D. S.-K., and Fartaj, A., "Aerodynamic Models for Darrieus-Type Straight-Bladed Vertical Axis Wind Turbines," *Renewable and Sustainable Energy Reviews*, Vol. 12, No. 4, 2008, pp. 1087–1109.
- <sup>7</sup>Sheldahl, R. E. and Klimas, P. C., "Aerodynamic Characteristics of Seven Symmetrical Airfoil Sections through 180-Degree Angle of Attack for Use in Aerodynamic Analysis of Vertical Axis Wind Turbines," Tech. rep., Sandia National Laboratories, Albuquerque, NM (USA), 1981.